12-2018

Finite Element Method Analysis of Whispering Gallery Acoustic Sensing

T. Le
Portland State University

H. Tran
Portland State University

Rodolfo Fernandez Rodriguez
Portland State University, rodolfo.f.r@gmail.com

C.J. Solano Salinas
National University of Engineering, Lima, Perú

Nima Laal
Portland State University, nima.laal@gmail.com

See next page for additional authors

Citation Details

Le, T., Tran, H., Fernandez, R., Salinas, C. S., Laal, N., Bringas, R., ... & La Rosa, A. H. (2018, December). Finite element method analysis of whispering gallery acoustic sensing. In Journal of Physics: Conference Series (Vol. 1143, No. 1, p. 012014). IOP Publishing.

Finite element method analysis of whispering gallery acoustic sensing

IOP Conf. Series: Journal of Physics: Conf. Series **1143** (2018) 012014 doi:10.1088/1742-6596/1143/1/012014

Finite element method analysis of whispering gallery acoustic sensing

T Le[1], H Tran[1], R Fernandez[1], C J Solano Salinas[2], N Laal[1], R Bringas[2], J Quispe[2], F Segundo[2] and A H La Rosa[1]

[1]Portland State University, Portland, Oregon 97201, USA
[2]National University of Engineering, Facultad de Ciencias, Lima, Perú

E-mail: thanh4@pdx.edu, andres@pdx.edu

Abstract. Whispering Gallery Acoustic Sensing (WGAS) has recently been introduced as a sensing feedback mechanism to control the probe-sample separation distance in scanning probe microscopy that uses a quartz tuning fork as a sensor (QTF-SPM) [1]. WGAS exploits the SPM supporting frame as a resonant acoustic cavity to monitor the nanometer-sized amplitude of the QTF oscillations. Optimal WGAS sensitivity depends on attaining an exact match between the cavity's frequency peak response and the TF resonance frequency. However, two aspects play against this objective: *i*) the unpredictable variability of the TF resonance frequency (upon attaching a SPM-probe to one of its tines), and *ii*) cavities of arbitrary geometry tend to display complicated (multiple peaks) frequency response, making difficult to identify which cavity dimension control which peak. Practical matching frequency procedures are needed then to operate the Shear-force Acoustic Near-field Microscopy (SANM) more efficiently. As a first step, here we undertake finite-element method (FEM) analysis to find out cavities of simple frequency response and, ideally, easy frequency tuning ability. Based on previous results we focus our studies in analyzing the frequency response of conical cavities within a range around the 32 kHz operating frequency. To first validate our numerical simulation studies, we reproduce the experimental results obtained from a specific conical cavity. Then we proceed to simulate the response of cavities of slightly different geometries, and investigate the dependence on the young modulus, poison ratio, and slight changes in dimensions. This initial success encourages to undertake studies of cavities having more sophisticated geometries.

1. Introduction

Whispering Gallery Acoustic Sensing (WGAS) [1] constitutes a simple, low-cost, and still effective, way to implement probe-sample distance feedback control in scanning probe microscopy (SPM). A critical step in SPM is to count with a sensing mechanism (the control signal) that varies monotonically with the probe-sample distance. In Scanning Tunneling Microscopy the control signal is the tunneling current across the probe-sample gap [2]; in Atomic Force Microscopy it is the contact force exerted by the surface on the probe [3]; in QTF-SPM it is the electrical piezoelectric current caused by the electrically driven, lateral oscillation of the quartz tuning fork (QTF) sensor [4]. All these approaches have their advantages and disadvantages. The simplicity of the WGAS, and hence its low cost implementation, lies in exploiting the SPM support-frame as a resonant acoustic cavity to monitor the oscillatory motion of a distant QTF. In the interpretation suggested in Fig. 1a and 1b, the nanometer-sized lateral oscillations of the QTF-tines

generates acoustic waves on the holding central shaft. Upon reaching the upper region, the sound waves then spread across the walls of the cavity, and standing waves are established. By judiciously placing an acoustic transducer on the perimeter of the cavity for maximum signal detection, WGAS is able to monitor the nanometer-size oscillations of the probe. Fig. 1c shows the cavity acoustic response (magnitude and phase) when the QTF is electrically excited (external source not shown) at different frequencies near the QTF resonance frequency. At resonance, typical values of the QTF amplitude is 10 nm.

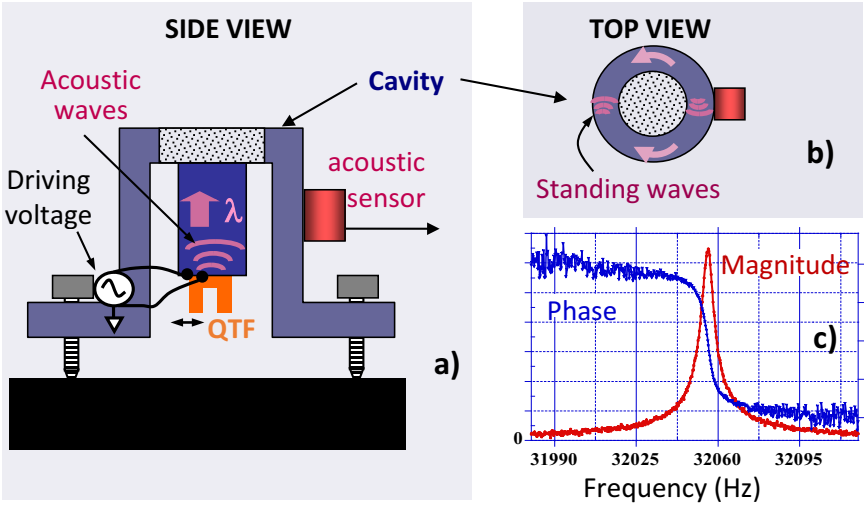

Figure 1. Suggested WGAS working principle mechanism: ***a)*** The nanometer-sized lateral oscillations amplitude of an electrically driven QTF establishes acoustic waves that propagate first upwards and ten towards the cavity; ***b)*** Standing waves are established on the cavity, and an acoustic sensor is placed at a position of maximum acoustic response; ***c)*** Cavity's acoustic response as the QTF is excited across its mechanical resonance frequency.

WGAS acoustic signal can be exploited in SPM by attaching a sharp stylus to one of the tines of a QTF. While driving the QTF (with the probe attached) at its resonance frequency, the probe is brought in close proximity to a sample (Fig. 2a). As a result of the probe-sample interaction, the QTF amplitude of oscillations decreases, which causes also the WGAS signal to decrease monotonically (Fig. 2b) as the probe-sample distance decreases. The latter feature makes WGAS suitable to be used as a feedback control signal. This capability—complemented with lateral scanning of the probe across the sample—allows characterization of the sample topography, as demonstrated in Fig. 2c.

Maximum sensitivity in WGAS would be obtained under ideal perfect match between the cavity's resonance frequency and the probe's mechanical resonance frequency. But the latter seldom occurs (see Fig. 3) because of *i*) the variability of the QTF resonance frequency upon attaching a SPM probe to one of its tines, and *ii*) the typically complicated spectral response of the cavity (displaying multiple peaks, and no clarity on which dimension affects which peak). A potential solution consists in adding a small mass to the QTF [5]; but it carries a consequent loss in sensitivity any time glue is added to the probe. Another potential solution is to model analytically the SPM frame and identify stable resonance peaks (*i.e.* those that do not change dramatically with the cavity dimensions), so a cavity could be built accordingly. But, lack of symmetry in typical SPM-heads makes the analytical equations very difficult to solve. In addition, a variety of bulk and surface acoustic waves can be excited in a given non-homogeneous and non-symmetrical cavity

[6]. As an alternative, we propose to use finite-element method (FEM) to analyze cavities of arbitrary geometries and dimensions.

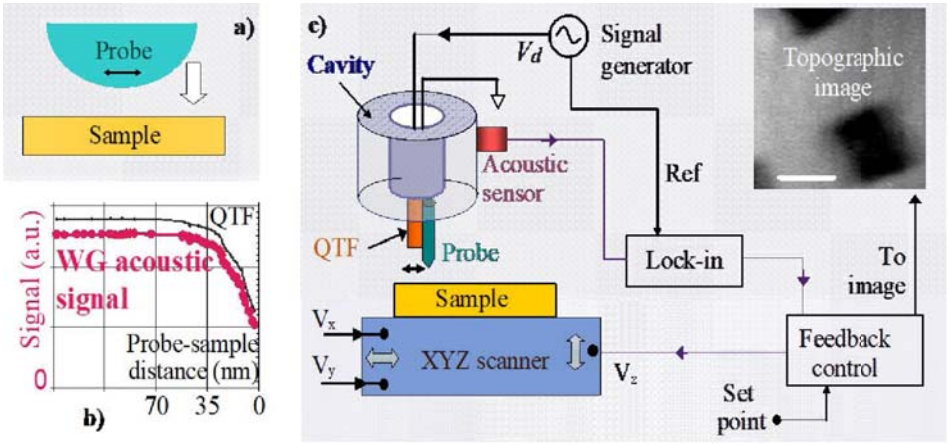

Figure 2. WGAS as a feedback signal-control for acquiring topographic images. When the probe approaches the sample **(a)**, the WGAS signal decreases monotonically when is close to the sample surface **(b).** The latter is exploited for feedback control and generate topographic image of the sample surface **(c)** [1].

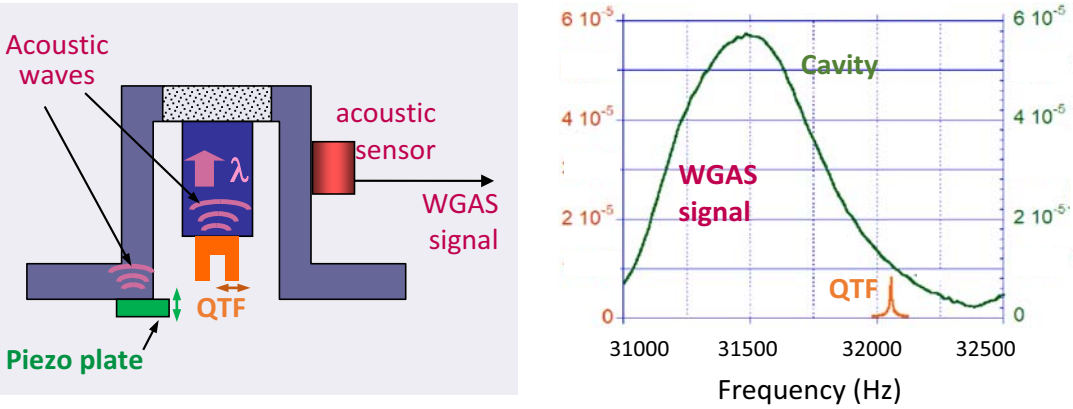

Figure 3. **Left:** Cavity excited by either a piezo plate or by the QTF within a narrow bandwidth (electrical driving sources not shown). **Right:** WGAS signal responses to the corresponding excitations. Notice the mismatch between the cavity's frequency response and the QTF resonance. In this paper we explore ways to slightly modify a cavity to match its frequency response with the QTF's resonance frequency.

Herein we report our preliminary results using FEM to analyze the frequency response of a conic-cylindrical cavity. The use of this geometry responds to the fact that in previous measurements [5] we found that such a cavity exhibits a well isolated frequency response near 32 kHz; which should simplify the FEM study approach. Still, it was unknown whether or not it was very sensitive to

changes of the cavity's properties. This paper embraces such a pending task, and testing in addition the dependence of the frequency-peaks on the material's Young's modulus and Poisson's ratio. Further, to explore the possibility of enabling tunable-frequency capability into the cavity, the FEM analysis will include the effect of adding small rings of different thicknesses to the conical cavity.

2. Effects of Material Properties on the Spectral Response

2.1 Cavity geometry and the simulation procedure

Previous experimental measurements on cavities of cylindrical-type shape [5] revealed that cavities with conical shape display a relatively simpler spectral response (isolated peaks, lower number of spectral peaks). The conical taper appears to 'discard' some peaks that otherwise would be present if the cavity were vertically straight. A conical cavity results then suitable to investigate how a particular frequency peak depends on the physical parameters, size, and slight changes in geometry. Accordingly, we have selected a cylindrical conical cavity for the current studies. Fig. 4 shows a 3D view, vertical cross section and dimensions of the actual cavity used here for both experimental tests and simulation calculations.

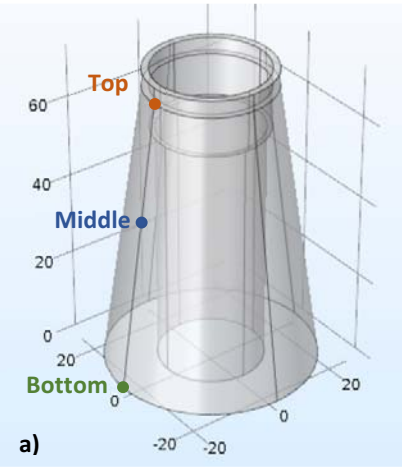

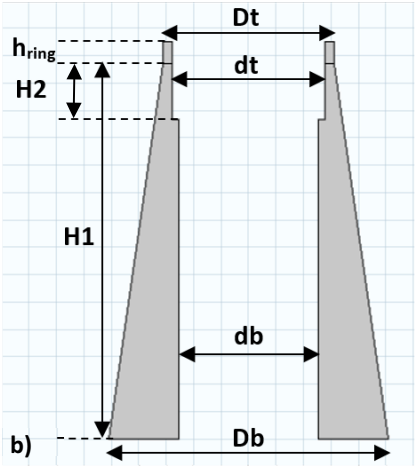

Dimension	Value (mm)
Db	53.6
Dt	31.2
db	27.8
dt	25.4
H1	68.5
H2	10.2
h_{ring}	vary

c)

Figure 4. Conical cavity used in FEM simulations: **a)** 3D view schematic of the actual cavity (top ring added) with the three positions where the acoustic sensor is located. **b)** Cross section view; **c)** Cavity dimensions table.

The structural mechanics module from COMSOL Multiphysics is used to solve the partial differential equations that govern the mechanical behavior of the cavity. The detailed geometry is designed in the COMSOL in order to minimize the meshing error in structural mechanics simulation. An appropriate discrete mesh for the simulation is selected, a task greatly simplified by the default physics-controlled meshing sequences available within the software package. Selection of the "fine" meshing option offers a good compromise between simulation accuracy and computing memory resources. The final free tetrahedral mesh has maximum element size of 5.64 mm and minimum element size of 0.70 mm.

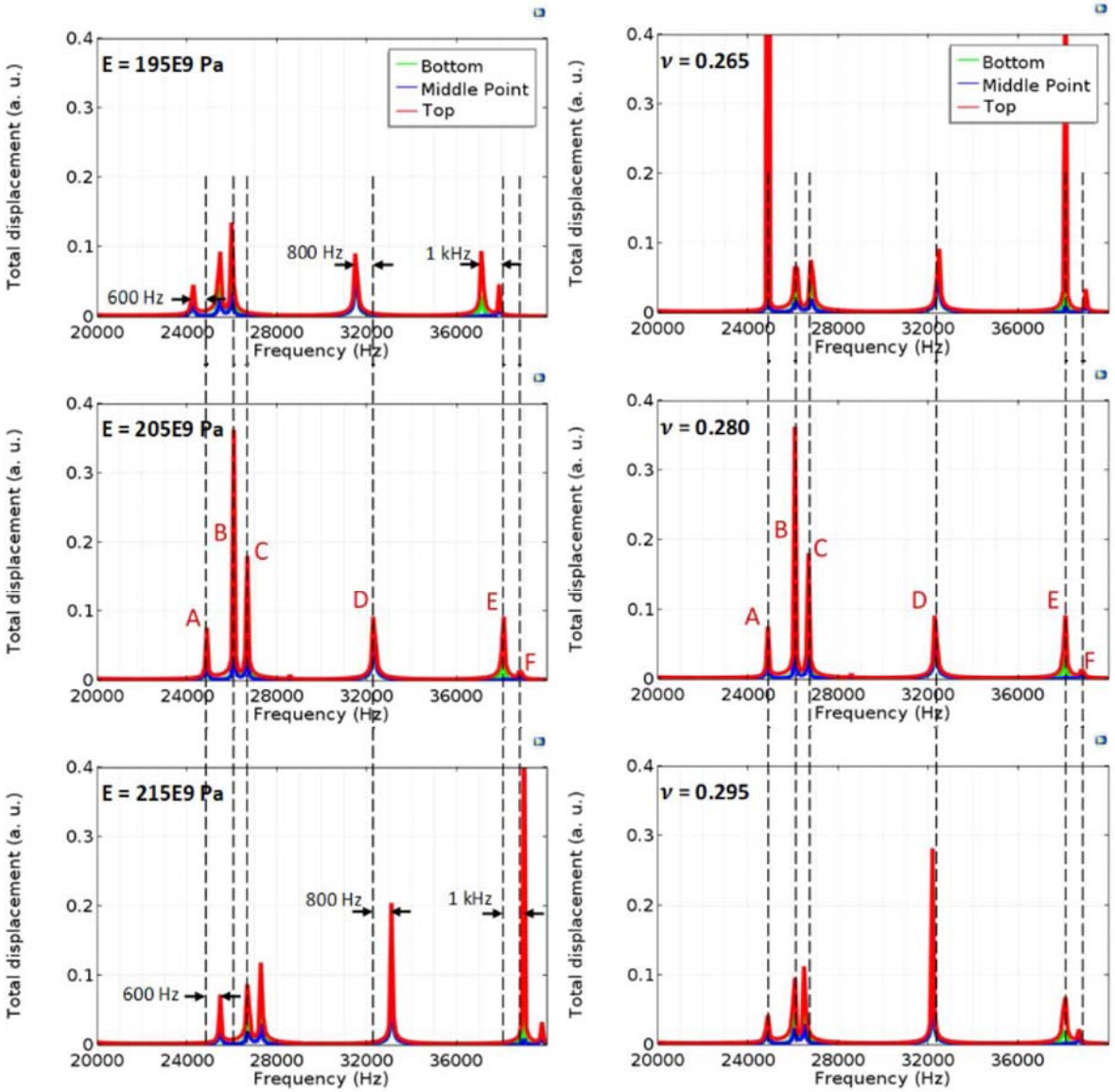

Figure 5. The frequency spectrum variation for 5% change in: **a)** Young's modulus and **b)** *Poisson*'s ratio.

The partial differential equations for the elastic wave inside solid structures were projected onto finite spaces using Solid Mechanic Module. A point load is added at the base of cavity to serve as the excitation source (mimicking the actual piezo plate use to excite the actual cavity.) The point excitation force is set to have equal amplitude along the Ox, Oy and Oz axes. The selected frequency domain of study is 20 kHz to 40 kHz. In all the results presented below (Figs. 5 to 7), three spectra are plotted together in the same graph, corresponding to three different positions of the sensor (top, middle and bottom). The general trends are that the intensity of the peaks changes with the sensor position, but there is no change in the peaks spectral position.

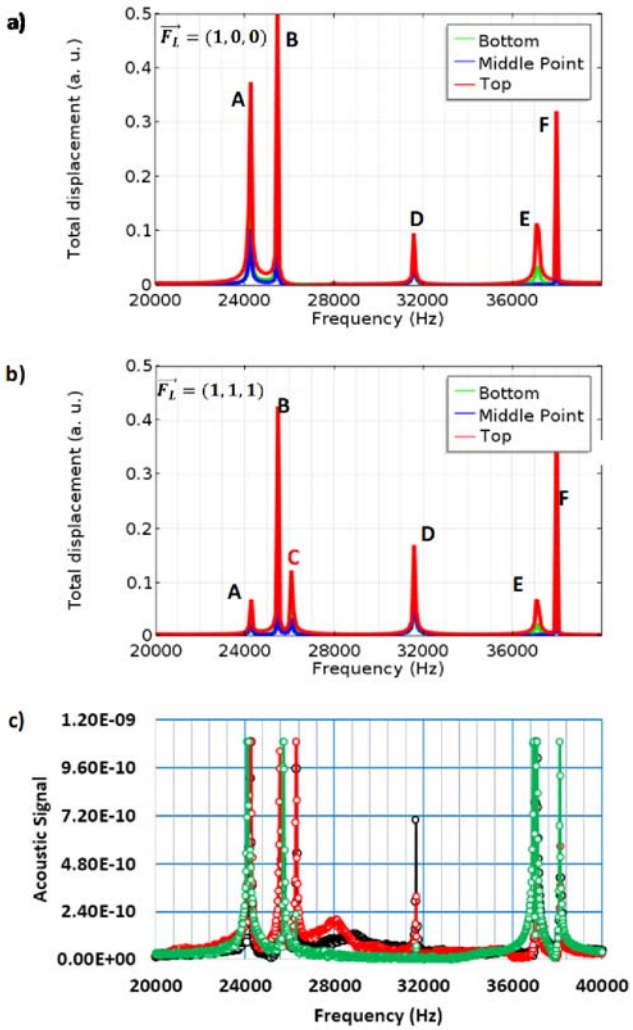

Figure 6. Superimposed spectra obtained with the acoustic sensor placed at different arbitrary positions on the external periphery of the conical cavity. **Bottom spectrum c)** Experimental results. Cavity is excited by an external piezoelectric plate placed at the base. Notice that in some traces peak "C" is missing. **Top spectra:** Simulations with a point source excitation (F_L) located at the cavity base **a)** $\mathbf{F_L}$ along the horizontal axis; **b)** $\mathbf{F_L}$ along (x,y,z) axes.

2.2 Sensitivity of the cavity's frequency response to changes in the material properties

Due to the different fabrication processes of the cavity material, there will be an uncertainty on the exact values of the cavity's physical properties, namely the Young's modulus and the Poisson's ratio. To evaluate the sensitivity of the cavity's spectral response to these properties, we perform simulations with nominal values of 205 $\times 10^9$ Pa for the Young's modulus and 0.28 for the Poisson's ratio and allowing $\pm$ 5% uncertainty [7]. The results are shown in Fig. 5. Notice all the peaks move consistently to the right with increasing values in the Young's modulus (Fig. 5a), with the peaks of higher frequency shifting by a slightly

larger amount (peak A shifts by 600 Hz, peak D shifts by 800 Hz, and peak E shifts by 1000 Hz.) On the other hand, the spectra do not change substantially with increasing values of the Poisson's ratio (Fig. 5b).

2.3 Matching simulation calculations with experimental results

A good agreement between experimental and simulation results is obtained when using a Young's modulus of 195×10^9 Pa and a Poisson's ratio of 0.27 (Fig. 6). Again, the intensity of the peaks changes with different sensor positions, but the peaks spectral position stays the same. Notice in Fig. 6a that peak "C" is absent, which can be attributed to the fact that the excitation point source (placed at the base of the cavity) was selected to oscillates purely in the horizontal direction. In contrast, the results in Fig. 6b correspond to the point source oscillating along the (1, 1, 1) direction; the additional yz-component excitation results in the appearance of the extra peak "C" in the spectrum.

3. Analysis of the geometrical cavity dimension effect on the Spectral Response

3.1 Sensitivity of the frequency response to 100-micron changes in cavity dimensions

Here we report on the sensitivity of peaks' position in the spectra to changes in the cavity dimensions (Table 1). The values are considered to increase by 100 microns, which is a precision fairly achieved in a CNC lathe machine.

Table 1: Frequency changes (in Hz) when each dimensions is increased by 100 microns.

Dimension (mm)	Peak A 24.3 kHz	Peak B 25.5 kHz	Peak C 26.2 kHz	Peak D 31.6 kHz	Peak E 37.1 kHz	Peak F 38.0 kHz
Cone height (H1)	20	10	-30	-20	60	0
Top hollow height (H2)	20	-30	-60	-30	50	-50
Cone base diameter (Db)	-30	-40	-40	-20	-40	-40
Cone top diameter (Dt)	-10	0	0	0	-20	10
Hollow bottom diameter (db)	0	50	30	10	-40	40
Hollow top diameter (dt)	-100	-20	0	-40	-80	-20

3.2 Sensitivity of the frequency response to slight modification in cavity geometry

In order to obtain the effect of changing the geometry of the cavity on the spectral response, we performed two modifications. The first modification is simulations with different taper angle (1^o change) geometries by keeping the same height (H1) then changing the conical base diameter (Db). Fig. 7a shows the results when Db is increased, which results in a decrease in the cone angle. The simulations with gradually smaller cone-angle (1^o precision) allowed discriminating the peaks in two distinct groups: (A, B, C, E) with a tendency towards a "blue" shift, and (D, F) with a tendency towards a "red" shift. In the first group, peak E is the one that is sensitive the most (1.5 kHz per degree first, then 0.5 kHz per degree), while the group of peaks A, B, and C undergo a smaller shift (peak-A shift 1 kHz first and then 0.5 kHz per degree). On the other hand, the second group comprises peaks (D and F) that do not shift significantly. The position of peak F, for example, is practically immune to the cone-angle variations, while peak D displays at most a slight "red" shift of less than 200 Hz per degree. These results suggest *a*) peak E to be greatly influenced by the length along the cone (the steeper the cone, the smaller taper length, the greater the frequency), and *b*) peak frequencies D and F to be associated to the inner diameter of the cavity (a parameter that was not changed during these simulations).

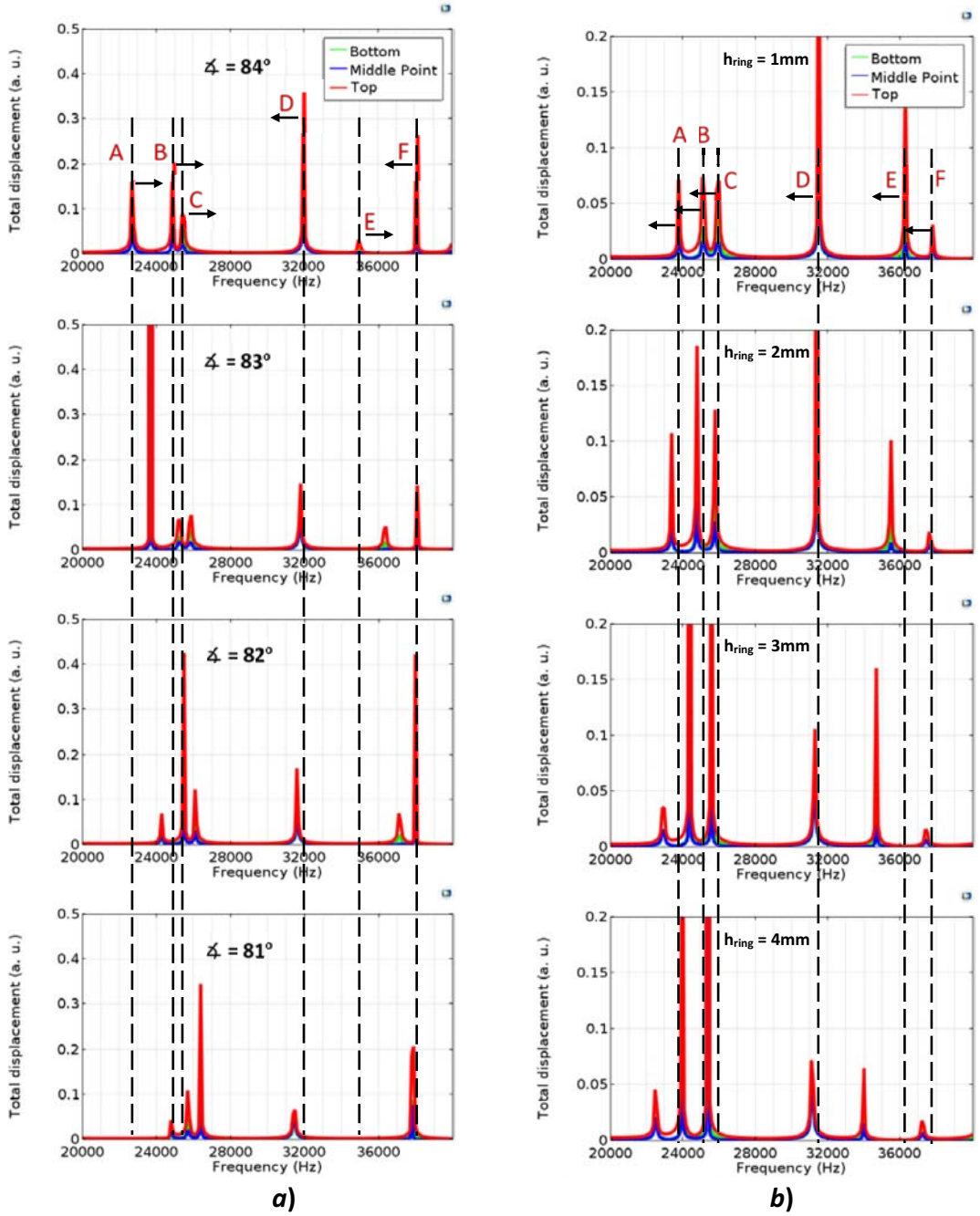

Figure 7. Spectral response variations as ***a)*** the cone angle of the cavity increases, and ***b)*** when adding rings of different thicknesses (h_{ring} in Fig. 4) to the top of the cavity.

Second, we modified the structure by adding hollow rings of different thickness to the top of the original cavity. Fig. 7b corresponds to the case in which a ring of variable thickness (h_{ring}) were added. Notice all the peaks undergo a "red" shift as the thickness of the ring increases. Frequency shifts of the order of 100

Hz were obtained for rings of 1 mm thickness. The peaks are discriminated in a similar fashion as when the cone angle changes: the (A, B, C, E) group has peaks E and A highly sensitive to the added perturbations, while the peaks D and F are minimally perturbed. Since peak D appears immune to the changes in the base and the height of the rings, it is plausible to associate this peak to the internal diameter.

4. Conclusions

Finite-element method (FEM) was used to study the structural frequency response of a stainless steel conical-cylinder cavity of dimensions typically used in actual Shear-force Acoustic Near-field Microscopy (SANM) settings. The cavity was purposely separated from the full SANM-frame design to simplify our preliminary FEM studies. As a preliminary step we verified changes in the cavity's spectral response for *i*) 5% uncertainty in the materials physical properties (Young modulus and Poisson's ratio), and *ii*) 100 m uncertainty in the different cavity dimensions.

First, we validated our simulation calculations by being able to reproduce experimental measurements performed on a hollow truncated-cone cavity. In preliminary simulations, the cavity was excited by a point-source oscillating along one-component shear excitation axis. In those cases, an initial discrepancy existed between the simulated and experimental results. Indeed, there was a particular peak consistently missed in the simulated spectra, which was also missing in some other spectra measurements. The discrepancy was resolved by incorporating both a shear and longitudinal excitation in the simulation, after which the simulations reproduced closely all the experimental peaks. This finding illustrate one of the advantages offered by FEM, helping to discriminate peaks based on the excitation modality.

Next, tests with different cone angles provide insights to take into consideration in the design and construction of SANM cavities. However, it is also necessary to explore solutions that can permit SANM users to in situ match the cavity's frequency response to the resonance frequency of the QTF (the uncertainty in the latter is caused by the stylus attached to one of its tines). A suggested practical solution considers adding small rings with different thickness on the top of the cavity and the simulation result support this approach. This way the SANM user would be able to modify the cavity in the act. Complementary tests for further verification of these hypotheses are currently underway.

In short, compared to the task of exploring analytical solutions of frequency response to arbitrary modifications of a cavity, the FEM analysis offers an alternative simpler approach. The ability of FEM to reproduce experimental results, as demonstrated here, constitutes an encouraging first step.

Bibliography

[1] La Rosa A H, Li N, Fernandez R, Wang X, Nordstrom R, and Padigi S K 2011 *Rev. Sci. Instrum.* **82**, 093704
[2] Chen C J, *Introduction to Scanning Tunneling Microscopy*, 2nd edition. Oxford: Oxford University Press, 2016
[3] Lanza M *Conductive Atomic Force Microscopy: Applications in Nanomaterials*. John Wiley & Sons, 2017
[4] Polesel-Maris J, Lubin C, Thoyer F, and Cousty J 2011 *J. Appl. Phys.* **109** 74320
[5] Hung H-C, La Rosa A H, Fernandez R, Comnes B, and Nordstrom R 2014 *SOP Trans. Appl. Phys.* **1** 22
[6] Ventsel E and Krauthammer T 2001 *Thin Plates and Shells: Theory: Analysis, and Applications*. CRC Press
[7] Overview of materials for Stainless Steel. Available online: http://www.matweb.com/search/datasheet.aspx?MatGUID=71396e57ff5940b791ece120e4d563e0&ckck=1.